

---

# GEM-2: NEXT GENERATION MOLECULAR PROPERTY PREDICTION NETWORK WITH MANY-BODY AND FULL-RANGE INTERACTION MODELING

---

A PREPRINT

**Lihang Liu**<sup>\*</sup>

Baidu Inc.

liulihang@baidu.com

**Donglong He**<sup>\*</sup>

Baidu Inc.

hedonglong@baidu.com

**Xiaomin Fang**<sup>†</sup>

Baidu Inc.

fangxiaomin01@baidu.com

**Shanzhuo Zhang**

Baidu Inc.

zhangshanzhuo@baidu.com

**Fan Wang**<sup>†</sup>

Baidu Inc.

wang.fan@baidu.com

**Jingzhou He**

Baidu Inc.

hejingzhou@baidu.com

**Hua Wu**

Baidu Inc.

wu\_hua@baidu.com

August 12, 2022

## ABSTRACT

Molecular property prediction is a fundamental task in the drug and material industries. Physically, the properties of a molecule are determined by its own electronic structure, which can be exactly described by the Schrödinger equation. However, solving the Schrödinger equation for most molecules is extremely challenging due to long-range interactions in the behavior of a quantum many-body system. While deep learning methods have proven to be effective in molecular property prediction, we design a novel method, namely GEM-2, which comprehensively considers both the long-range and many-body interactions in molecules. GEM-2 consists of two interacted tracks: an atom-level track modeling both the local and global correlation between any two atoms, and a pair-level track modeling the correlation between all atom pairs, which embed information between any 3 or 4 atoms. Extensive experiments demonstrated the superiority of GEM-2 over multiple baseline methods in quantum chemistry and drug discovery tasks.

**Keywords** Molecular property prediction · Many-body interactions · Long-range interactions

## 1 Introduction

Molecular property prediction is a fundamental task in drug and material industries, evaluating the physical, chemical, and biological properties to assist the researchers in making decisions. In essence, the properties of a molecule are determined by its own electronic structure. For example, the HOMO-LUMO gap of molecules is related to reactivity, photoexcitation, and charge transport Nakata and Shimazaki [2017]. Theoretically, the electronic structure of molecules can be exactly described by the Schrödinger equation. However, solving the Schrödinger equation for most molecules is extremely difficult, because a molecule with multiple electrons is a many-body system with quantum long-range interactions Defenu et al. [2021].

After decades of endeavours, computational chemists have developed a variety of calculation methods to approximate the solution of Schrödinger equation. The two representative ones are density functional theory (DFT) and coupled-cluster theory (CC). The core idea of DFT is to represent all electrons with a single electron density, thus reduces the dimension of the problem Burke and Wagner [2013]. However, the error of DFT is significant because of the limited accuracy of the selected functional, which can be improved by using functionals considering long-range interactions

---

<sup>\*</sup>Equal contribution

<sup>†</sup>Corresponding authors

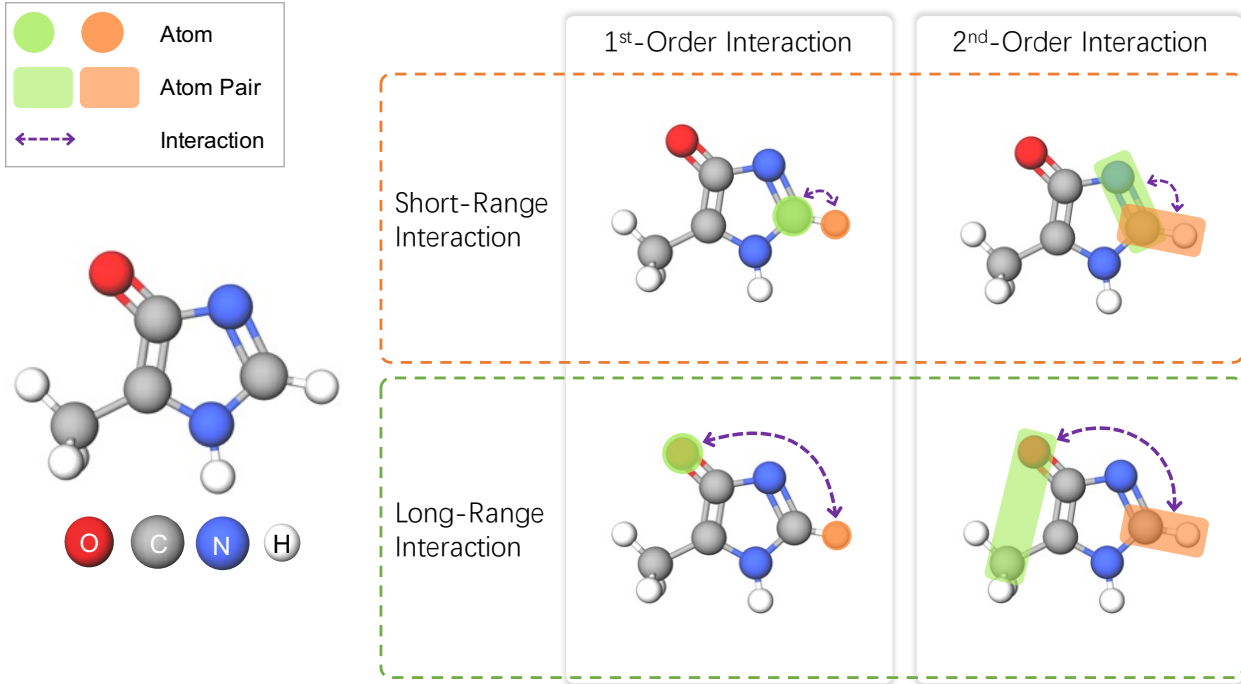


Figure 1: Two Dimensions of molecular interaction. One is whether the many-body interaction is consider, which can be further categorized into the 1<sup>st</sup>-order interaction of atoms, the 2<sup>nd</sup>-order interaction of atom pairs, and to infinite order. The other one is whether the long-range interactions of particles is considered. In the long-range scenario, any two atoms or atom pairs can directly interact with each other.

and/or hybrid functionals with higher-order gradient terms Peverati and Truhlar [2014]. The CC is currently regarded as the gold standard for many quantum problems Bertels et al. [2021]. The calculation of CC is based on an exact solution of the ground state of the system, and is further stacked with a series of cluster operators to approximate the interactions between all electrons. These cluster operators can be extended from single and/or double to infinite order to increase the accuracy Zhang and Grüneis [2019].

Owning to the great success of deep neural networks (DNNs) in broad fields, many studies attempted to adopt the widely used models to predict molecular properties. Inspired by the calculation methods of Schrödinger equation, we have classified the existing methods in two dimensions: the first is whether the many-body interactions is considered, and the second is whether the long-range interactions of particles is considered. For the first dimension, since we realize that most of the existing work adopted a message passing framework or its variants to model the interactions between atoms, we re-define the interactions between atoms as the 1<sup>st</sup>-order interactions (describes the 2-body interactions), and the interactions between atom pairs as the 2<sup>nd</sup>-order interactions (describes the 3- or 4-body interactions). Like the CC, the interactions modeling framework can be extended to infinite order. While for the second dimension, we can categorize current works into two types by the range of interactions. One is the GNN-based methods that only consider the short-range interactions of local neighborhoods, for example, atoms or atom pairs only interact with those that are spatially close to each other. In this way, the dependency of two highly-correlated but far-apart atoms or atom pairs has to be inferred inefficiently through the step-by-step message-passing manner. The other one is Transformer-style architectures that model the full-range interactions, including both short- and long-range interactions. These architectures directly learn the global dependency through the fully-connected attention mechanism. An overall summary of current deep learning works by these two dimensions can be viewed in Table 1.

Although increasing studies have noticed the importance of many-body interaction and long-range interaction for molecular modeling, designing a principled model architecture that can comprehensively integrate these two factors still requires in-depth investigation. To this end, we propose a novel molecular modeling architecture, GEM-2, which considers not only many-body but also long-range interaction. The architecture of GEM-2 consists of two tracks: an atom-level track for capturing the full-range 1<sup>st</sup>-order interactions between any two atoms and a pair-level track for capturing the full-range 2<sup>nd</sup>-order interactions between any two atom pairs, which involves 3 or 4 atoms. We design a pair-aware self-attention mechanism for the atom-level track to learn the global dependency within atoms. Besides, considering the computational efficiency, we adopt Triangular Self-Attention attention Jumper et al. [2021] for the

pair-level track to learn the global dependency between pairs. Meanwhile, The atom-level track and the pair-level track also communicate with each other through the outer-product operator and the pair-aware self-attention.

To verify the effectiveness of GEM-2, we compare it with several competitive baselines on the tasks of quantum chemistry and drug discovery, where GEM-2 outperforms previous SOTA methods by a large margin. Our contributions can be summarized as follows:

- We propose a novel network architecture, GEM-2, which comprehensively integrates the many-body interaction and full-range interaction for molecular modeling.
- The model architecture of GEM-2 adopts various well-designed attention mechanisms to model the  $1^{st}$ -order interaction of atoms and the  $2^{nd}$ -order interaction of atom pairs, as well as the communication between atoms and atom pairs.
- Extensive experiments demonstrate that GEM-2 considerably outperforms competitive baselines on multiple datasets and effectively extracts the knowledge of many-body interaction and global dependency.

## 2 Methodology

### 2.1 Problem Formulation

Previous works tend to model a molecule as a graph with each edge to indicate the local interactions of two atoms. In order to comprehensively consider high-order interactions and long-range interactions, we extrapolate the previous definition and re-define a molecule as  $M = (\mathcal{A}, \mathcal{P}, \mathcal{T})$ . Here,  $i \in \mathcal{A}$  represents an atom,  $(i, j) \in \mathcal{P}$  represents an atom pair (i.e., interactions of two atoms), and  $(i, j, k) \in \mathcal{T}$  represents an atom triplet (i.e., interactions of three atoms), where  $1 \leq i, j, k \leq N$ , and  $N$  denotes the number of atoms. Given a molecule, our proposed method (GEM-2) takes the features of atoms ( $\{\mathbf{x}_i^{atom}\}$ ), such as atom type, the features of pairs ( $\{\mathbf{x}_{ij}^{pair}\}$ ), such as chemical bond and spatial distance between two atoms, and the features of triplets ( $\{\mathbf{x}_{ijk}^{triplet}\}$ ), such as angle formed by three atoms, as input to predict the corresponding molecular property. Those features are transformed into the initial representations of atoms, pairs, and triplets through embedding layer Emb():

$$\mathbf{a}_i^{(0)} = \text{Emb}(\mathbf{x}_i^{atom}), \mathbf{p}_{ij}^{(0)} = \text{Emb}(\mathbf{x}_{ij}^{pair}), \mathbf{t}_{ijk}^{(0)} = \text{Emb}(\mathbf{x}_{ijk}^{triplet}), \quad \mathbf{a}_i^{(0)} \in \mathbb{R}^{c_{atom}}, \mathbf{p}_{ij}^{(0)} \in \mathbb{R}^{c_{pair}}, \mathbf{t}_{ijk}^{(0)} \in \mathbb{R}^{c_{triplet}}, \quad (1)$$

where  $\{\mathbf{a}_i^{(0)}\}$ ,  $\{\mathbf{p}_{ij}^{(0)}\}$ , and  $\{\mathbf{t}_{ijk}^{(0)}\}$  denotes the initial representations of atoms, pairs, and triplets, respectively.

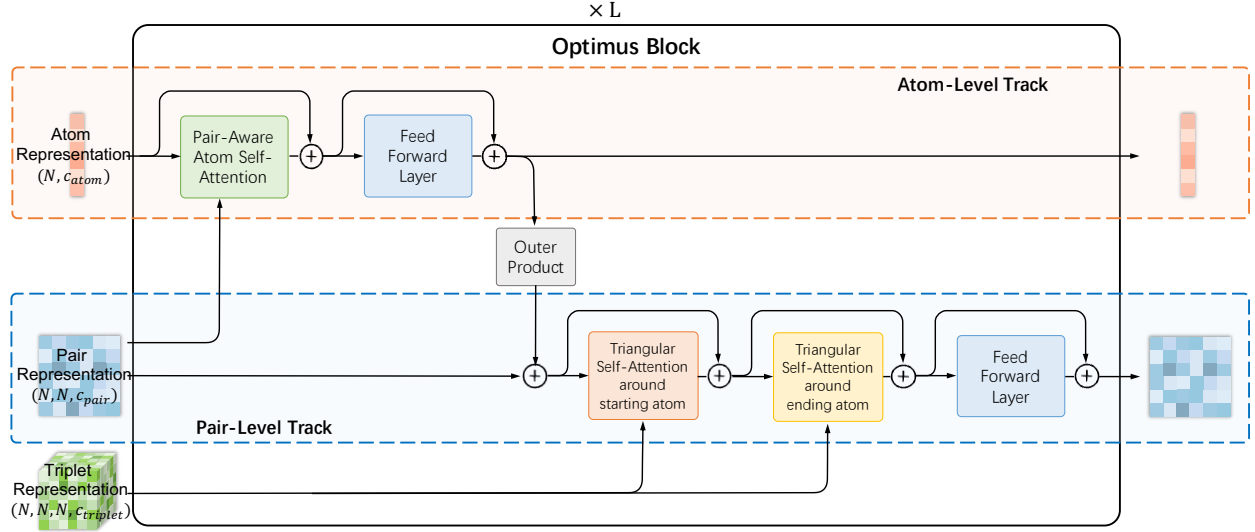
### 2.2 Overall Architecture

We design a novel network block, called Optimus, which serves as the main module of GEM-2, to model the first-order and second-order interactions of the molecules. GEM-2 contains  $L$  Optimus blocks, and each block's output is added via a residual connection. As shown in Figure 2a, the  $l$ -th Optimus block takes atom representation  $\mathbf{a}_i^{(l-1)}$ , the pair representation  $\mathbf{p}_{ij}^{(l-1)}$ , and triplet representation  $\mathbf{t}_{ijk}^{(l-1)} \in \mathbb{R}^{c_{triplet}}$  as input. Then, it utilizes a atom-level track and a pair-level track to model the  $1^{st}$ - order interactions and the  $2^{nd}$ - order interactions, respectively. The atom-level track mainly adopts the well-designed pair-aware self-attention mechanism to model the interactions between two atoms. For the pair-level track, Triangular Self-Attention mechanism is applied to learn the interactions between two atom pairs. Besides, pair-aware atom self-attention and outer product are adopted to exchange the information of the atom representations and pair representations between the atom-level track and the pair-level track. Finally, the Optimus block outputs the updated atom representation  $\mathbf{a}_i^{(l)}$  and pair representation  $\mathbf{p}_{ij}^{(l)}$ . Note that, the Optimus blocks would not update the triplet representation, i.e.,  $\mathbf{t}_{ijk}^0 = \mathbf{t}_{ijk}^{(1)} = \dots = \mathbf{t}_{ijk}^{(L)}$ . The whole process of Optimus is described in Algorithm 1. Average pooling is applied to the representations of all the atoms  $\{\mathbf{a}_i^{(L)}\}$  at the last Optimus block to obtain the representation of the whole molecule  $\mathbf{m}$ . Then, the molecular representation is feed into a Multilayer Perceptron (MLP) to predict the property.

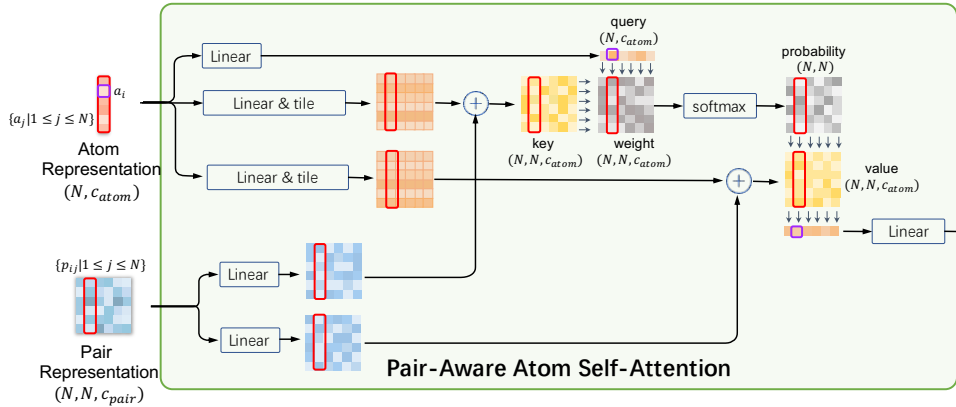
### 2.3 Atom-Level Track

The atom-level track aims to model the  $1^{st}$ -order interactions, i.e., the interactions between the atoms. Two layers, including a pair-aware atom self-attention and a feed forward layer, are connected through a residual operator.

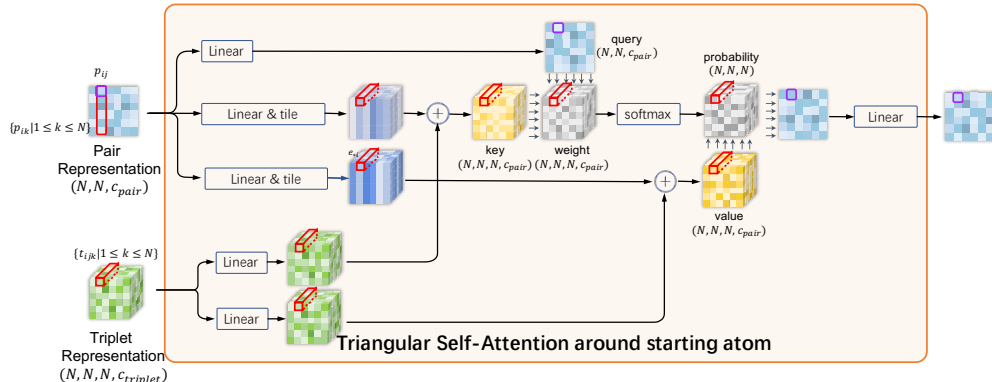
Previous works Ying et al. [2021], Dwivedi and Bresson [2020], Hussain et al. [2021a] tend to assume that when the pair information (i.e., spatial distances and chemical bonds) of atom pairs  $(i, j)$  and  $(i', j')$  are the same, they will have



(a) Overall architecture of Optimus block. It consists of an atom track colored in orange and a pair track colored in blue. And in between is the Outer Product layer for message exchange.



(b) Details of pair-aware atom self-Attention layer. This is a designed self-attention module to update atom representation by fusing messages from both atom representation and pair representation.



(c) Details of triangular self-attention around starting atom. This is a designed self-attention module to update pair representation by fusing messages from both pair representation and triplet representation.

Figure 2: GEM-2

**Algorithm 1** Optimus block

---

```

def Optimus( $\{\mathbf{a}_i\}$ ,  $\{\mathbf{p}_{ij}\}$ ,  $\{\mathbf{t}_{ijk}\}$ ,  $c_{\text{atom}}$ ,  $c_{\text{pair}}$ ,  $c_{\text{outer}}$ ,  $N_{\text{head}}^{\text{atom}}$ ,  $N_{\text{head}}^{\text{pair}}$ ):
  1: # Atom-level track
  2:  $\{\mathbf{a}_i\} += \text{Dropout}_{p_{\text{atom}}}(\text{PairAwareAtomSelfAttention}(\{\mathbf{a}_i\}, \{\mathbf{p}_{ij}\}, c_{\text{atom}}, N_{\text{head}}^{\text{atom}}))$ 
  3:  $\{\mathbf{a}_i\} += \text{Dropout}_{p_{\text{atom}}}(\text{FeedForward}(\{\mathbf{a}_i\}, c_{\text{atom}} * 4))$ 
  4: # Interaction between atom- and pair-level track
  5:  $\{\mathbf{p}_{ij}\} += \text{Dropout}_{p_{\text{pair}}}(\text{OuterProduct}(\{\mathbf{a}_i\}, c_{\text{outer}}, c_{\text{pair}}))$ 
  6: # Pair-level track
  7:  $\{\mathbf{p}_{ij}\} = \text{LayerNorm}(\{\mathbf{p}_{ij}\})$ 
  8:  $\{\mathbf{p}_{ij}\} += \text{Dropout}_{p_{\text{pair}}}(\text{TriangularAttentionStartingAtom}(\{\mathbf{p}_{ij}\}, \{\mathbf{t}_{ijk}\}, c_{\text{pair}}, N_{\text{head}}^{\text{pair}}))$ 
  9:  $\{\mathbf{p}_{ij}\} += \text{Dropout}_{p_{\text{pair}}}(\text{TriangularAttentionEndingAtom}(\{\mathbf{p}_{ij}\}, \{\mathbf{t}_{ijk}\}, c_{\text{pair}}, N_{\text{head}}^{\text{pair}}))$ 
 10:  $\{\mathbf{p}_{ij}\} += \text{Dropout}_{p_{\text{pair}}}(\text{FeedForward}(\{\mathbf{p}_{ij}\}, c_{\text{pair}} * 4))$ 
 11: return  $\{\mathbf{a}_i\}$ ,  $\{\mathbf{p}_{ij}\}$ 

```

---

the same effects on the interactions of those atom pairs. More concretely, when modeling the interaction from atom  $j$  to atom  $i$ , previously adopted attention mechanisms regard the information of atom pair  $(i, j)$  as a bias than is transformed from the pair representation ( $b_{ij} = \text{Linear}(\mathbf{p}_{ij})$ ) and add it to the attention weights, i.e.,  $\alpha_{ij} = \text{softmax}_j(\mathbf{q}_i^T \mathbf{k}_j + b_{ij})$  to adjust the strength of the interaction. However, such assumption is not so realistic. For example, suppose the distances of atom pair  $(i, j)$  and atom pair  $(i', j')$  are the same, their mutual forces could be different due to the different characteristics of atom  $i$  and atom  $i'$  (atom  $j$  and atom  $j'$ ).

In order to fuse the pair information into the interaction between the atoms in a more reasonable way, we design the pair-aware atom self-attention, as shown in Figure 2b and Algorithm 2. Instead of regarding the pair information as the bias of the attention weights, we incorporate the pair information into the keys and values of the attention mechanism. Both the key  $\mathbf{k}_{ij}^h$  and the value  $\mathbf{v}_{ij}^h$  (line 5) combines the atom representation  $\mathbf{a}_i$  and pair representation  $\mathbf{p}_{ij}$ . Then, the attention weights (line 8) calculated by the pair-aware keys can benefit from the pair information. The pair-aware attention weights  $\alpha_{ij}^h$  as well as the pair-aware values  $\mathbf{v}_{ij}^h$  contribute to produce the updated atom representation (line 11).

**Algorithm 2** Pair-aware atom self-attention

---

```

def PairAwareAtomSelfAttention( $\{\mathbf{a}_i\}$ ,  $\{\mathbf{p}_{ij}\}$ ,  $c$ ,  $N_{\text{head}}$ ):
  1: # Input Projections
  2:  $\mathbf{a}_i = \text{LayerNorm}(\mathbf{a}_i)$ 
  3:  $\mathbf{p}_{ij} = \text{LayerNorm}(\mathbf{p}_{ij})$ 
  4:  $\mathbf{q}_i^h = \text{Linear}(\mathbf{a}_i)$ 
  5:  $\mathbf{k}_{ij}^h = \text{Linear}(\mathbf{a}_j) + \text{Linear}(\mathbf{p}_{ij})$ 
  6:  $\mathbf{v}_{ij}^h = \text{Linear}(\mathbf{a}_j) + \text{Linear}(\mathbf{p}_{ij})$ 
  7: # Attention
  8:  $\alpha_{ij}^h = \text{softmax}(\mathbf{q}_i^h \mathbf{k}_{ij}^h)$ 
  9:  $\mathbf{o}_i^h = \sum_j \alpha_{ij} \mathbf{v}_{ij}^h$ 
 10: # Output projection
 11:  $\hat{\mathbf{a}}_i = \text{Linear}(\text{concat}_h(\mathbf{o}_i^h))$ 
 12: return  $\{\hat{\mathbf{a}}_i\}$ 

```

---

## 2.4 Pair-Level Track

The pair-level track is designed to learn the 2<sup>nd</sup>-order interactions. Three layers, including two triangular self-attention layers and a feed forward layer are utilized to update the pair representations. Particularly, those two triangular self-attention layer exchange the messages within the atom pairs to model their interactions.

Similar to the pair-aware atom attention applied in the atom-level track, we design a novel attention mechanism to incorporate the triplet information into the modeling of interactions of atom pairs. Two triangular self-attention layers are introduced : 1) triangular self-attention around starting atom; 2) triangular self-attention around ending atom. In triangular self-attention around starting atom (Algorithm 3 and Figure 2c), atom pair  $(i, j)$  aggregates messages from atom pairs  $\{(i, k) | k=1^N\}$  that share the starting nodes with  $(i, j)$ . To be sensitive to the triplet representation, the keys

and the values combine the pair representation  $\mathbf{p}_{ij}$  and the triplet representation  $\mathbf{t}_{ijk}$ . Then, attention is applied on the triplet-sensitive keys and values to update the pair representations. Similarly, in triangular self-attention around ending atom (Algorithm 4), atom pair  $(i, j)$  aggregates messages from atom pairs  $\{(k, j) | k=1\}$  that share the ending nodes with  $(i, j)$ . The differences of the procedure of triangular self-attention around ending node to that of triangular self-attention around starting atom are marked with yellow background in Algorithm 4.

---

**Algorithm 3** Triangular self-attention around starting atom

---

```

def TriangularAttentionStartingAtom( $\{\mathbf{p}_{ij}\}$ ,  $\{\mathbf{t}_{ijk}\}$ ,  $c$ ,  $N_{\text{head}}$ ):
  1: # Input Projections
  2:  $\mathbf{p}_{ij} = \text{LayerNorm}(\mathbf{p}_{ij})$ 
  3:  $\mathbf{q}_{ij}^h = \text{Linear}(\mathbf{p}_{ij})$   $\triangleright \mathbf{q}_{ij}^h \in \mathbb{R}^c, h \in \{1, \dots, N_{\text{head}}\}$ 
  4:  $\mathbf{k}_{ijk}^h = \text{Linear}(\mathbf{p}_{ik}) + \text{Linear}(\mathbf{t}_{ijk})$   $\triangleright \mathbf{k}_{ijk}^h \in \mathbb{R}^c$ 
  5:  $\mathbf{v}_{ijk}^h = \text{Linear}(\mathbf{p}_{ik}) + \text{Linear}(\mathbf{t}_{ijk})$   $\triangleright \mathbf{v}_{ijk}^h \in \mathbb{R}^c$ 
  6: # Attention
  7:  $\alpha_{ijk}^h = \text{softmax}(\mathbf{q}_{ij}^T \mathbf{k}_{ijk}^h)$ 
  8:  $\mathbf{o}_i^h = \sum_k \alpha_{ijk} \mathbf{v}_{ijk}^h$ 
  9: # Output projection
 10:  $\hat{\mathbf{p}}_{ij} = \text{Linear}(\text{concat}_h(\mathbf{o}_i^h))$   $\triangleright \hat{\mathbf{p}}_{ij} \in \mathbb{R}^c$ 
 11: return  $\{\hat{\mathbf{p}}_{ij}\}$ 

```

---



---

**Algorithm 4** Triangular self-attention around **ending** atom

---

```

def TriangularAttentionEndingAtom( $\{\mathbf{p}_{ij}\}$ ,  $\{\mathbf{t}_{ijk}\}$ ,  $c$ ,  $N_{\text{head}}$ ):
  1: # Input Projections
  2:  $\mathbf{p}_{ij} = \text{LayerNorm}(\mathbf{p}_{ij})$ 
  3:  $\mathbf{q}_{ij}^h = \text{Linear}(\mathbf{p}_{ij})$   $\triangleright \mathbf{q}_{ij}^h \in \mathbb{R}^c, h \in \{1, \dots, N_{\text{head}}\}$ 
  4:  $\mathbf{k}_{ijk}^h = \text{Linear}(\mathbf{p}_{kj}) + \text{Linear}(\mathbf{t}_{ijk})$   $\triangleright \mathbf{k}_{ijk}^h \in \mathbb{R}^c$ 
  5:  $\mathbf{v}_{ijk}^h = \text{Linear}(\mathbf{p}_{kj}) + \text{Linear}(\mathbf{t}_{ijk})$   $\triangleright \mathbf{v}_{ijk}^h \in \mathbb{R}^c$ 
  6: # Attention
  7:  $\alpha_{ijk}^h = \text{softmax}(\mathbf{q}_{ij}^T \mathbf{k}_{ijk}^h)$ 
  8:  $\mathbf{o}_i^h = \sum_k \alpha_{ijk} \mathbf{v}_{ijk}^h$ 
  9: # Output projection
 10:  $\hat{\mathbf{p}}_{ij} = \text{Linear}(\text{concat}_h(\mathbf{o}_i^h))$   $\triangleright \hat{\mathbf{p}}_{ij} \in \mathbb{R}^c$ 
 11: return  $\{\hat{\mathbf{p}}_{ij}\}$ 

```

---

## 2.5 Message Exchanging between Atom Representations and the Pair Representations

The pair-aware atom self-attention in the atom-level track and out product are utilized to exchange the messages of atom representations and pair representations between the atom-level track and pair-level track. The pair representations are incorporated into atom representations through the pair-aware atom self-attention, while the atom representations play their roles in pair representations through outer product, as defined in Algorithm 5.

---

**Algorithm 5** Outer product

---

```

def OuterProduct( $\{\mathbf{a}_i\}$ ,  $c_{\text{outer}}$ ,  $c_{\text{pair}}$ ):
  1:  $\mathbf{a}_i = \text{LayerNorm}(\mathbf{a}_i)$ 
  2:  $\mathbf{m}_{ij} = \text{flatten}(\text{Linear}(\mathbf{a}_i) \otimes \text{Linear}(\mathbf{a}_j))$   $\triangleright \mathbf{m}_{ij} \in \mathbb{R}^{c_{\text{outer}} \cdot c_{\text{outer}}}$ 
  3:  $\hat{\mathbf{p}}_{ij} = \text{Linear}(\mathbf{m}_{ij})$   $\triangleright \hat{\mathbf{p}}_{ij} \in \mathbb{R}^{c_{\text{pair}}}$ 
  4: return  $\hat{\mathbf{p}}_{ij}$ 

```

---

Table 1: Classification of current works by the range and the order of interaction.

	1st-Order Interaction	Up-to-2nd-Order Interaction
Short-Range Interaction	SGCN Danel et al. [2020], Attentive FP Xiong et al. [2020], SchNet Schütt et al. [2017], DeeperGCN Li et al. [2020], Pre-trainGNN Hu et al. [2020], ...	D-MPNN Yang et al. [2019], DimeNet Klicpera et al. [2020], HMGNN Shui and Karypis [2020], GEM Fang et al. [2022], ...
Full-Range Interaction	MAT Maziarka et al. [2020], GT Dwivedi and Bresson [2020], SAN Kreuzer et al. [2021], CoMPT Chen et al. [2021], EGT Hussain et al. [2021a], ...	GEM-2

### 3 Related Work

As shown in Table 1, current molecular representations by deep neural networks can be categorized according to two dimensions: the first is whether the many-body interaction is considered, and the second is whether the long-range interaction is considered.

*Whether the many-body interaction is considered.* Based on the observation of current works, we re-define the many-body interaction into different orders. Since we realize that many existing works Danel et al. [2020], Xiong et al. [2020], Maziarka et al. [2020], Hussain et al. [2021a] regarding a molecule as a graph by taking atoms as nodes and chemical bonds as edges, we re-define such interaction as the 1<sup>st</sup>-order interaction between atoms. For example, Attentive FP Xiong et al. [2020] proposes to extend graph attention mechanism in order to learn aggregation weights during the atom interactions. Meanwhile, a bunch of studies have tried to incorporate 3D geometry information: Schütt et al. [2017], Li et al. [2021], Maziarka et al. [2020] take partial geometry information as features of atom pairs, such as atomic distances. As the 1<sup>st</sup>-order interaction between A few advanced works Klicpera et al. [2020], Yang et al. [2019], Shui and Karypis [2020] tried to incorporate 2<sup>nd</sup>-order interaction of atom pairs into the neural networks. Especially, our previous work GEM Fang et al. [2022] has demonstrated the positive effect of modeling high-order interactions for property prediction by building two graphs that are based on atoms and on atom pairs.

*Whether the long-range interaction is considered.* From this dimension, we can divide current works into two types: one is GNN-style networks that model short-range interaction and the other one is Transformer-style networks that model full-range interaction. GNNs Danel et al. [2020], Li et al. [2020], Hu et al. [2020] in nature model molecules as molecular graphs where atoms or atom pairs are connected only in the neighborhoods. For example, when building molecular graph, in Yang et al. [2019], Hu et al. [2020] two atoms are consider connected only if there are chemical bonds between them. While in the Klicpera et al. [2020], the atom pairs are connected if they are close in the spatial space. However, the GNN-based methods rely on the atoms' short-range interaction to infer the long-range interaction through the step-by-step message-passing technique. Such an indirect manner will likely harm the modeling of the dependency between the indirectly connected atoms, especially those far away. Therefore, leveraging Transformer-style architectures Maziarka et al. [2020], Dwivedi and Bresson [2020], Hussain et al. [2021a] to capture the full-range interaction has attracted increasing attention. For example, CoMPT Chen et al. [2021] proposed a Transformer variant by reinforcing message interactions between nodes and edges and introduced a message diffusion mechanism to leverage the graph connectivity inductive bias. And EGT Hussain et al. [2021a] proposed a residual edge channel as an extension to Transformer and introduced a generalized positional encoding scheme based on Singular Value Decomposition.

To sum up, although the importance of many-body and long-range interaction for molecular modeling has been noticed by increasing studies, designing a principled architecture that integrate these two dimensions still requires in-depth research.

### 4 Experimental Results

To thoroughly evaluate the performance of GEM-2, we compare it with multiple baseline methods on two kinds of molecular property prediction benchmarks, i.e., a quantum chemistry benchmark and a drug discovery benchmark. Then, ablation studies are conducted to investigate the impact of the short- / long-range as well as the 1<sup>st</sup>- / 2<sup>nd</sup>-order interactions.

Table 2: MAE scores of GEM-2 and multiple baselines on quantum chemistry dataset PCQM4Mv2.

Model	Validation	Test-dev
GCN Kipf and Welling [2017]	0.1379	0.1398
GIN Xu et al. [2019]	0.1185	0.1218
GCN-virtual	0.1153	0.1152
GIN-virtual	0.1083	0.1084
GRPE Park et al. [2022]	0.0890	0.0898
Graphomer Ying et al. [2021]	0.0864	-
EGT Hussain et al. [2021b]	0.0857	0.0862
GEM-2	<b>0.0793</b>	-

#### 4.1 Training Settings of GEM-2

GEM-2 takes the plenty of atom features, pair features, and triplet features as input (refer to Table 4 in Appendix for the feature list) for molecular property prediction. We train GEM-2 with Adam optimizer Kingma and Ba [2015], and exponential moving average (EMA) is used to smooth the model parameters to achieve more robust performance. Please refer to Table 5 for the detailed settings of the hyper-parameters.

#### 4.2 Results on Quantum Chemistry Benchmark

**Dataset.** PCQM4Mv2 is a large-scale quantum chemistry dataset, containing the DFT-calculated HOMO-LUMO energy gaps of the millions of molecules, which is originally curated under the PubChemQC project Nakata and Shimazaki [2017]. Open Graph Benchmark (OGB)<sup>3</sup> splitted the dataset according to their PubChem ID (CID) into training, validation, test-dev, and test-challenge sets with ratio 90:2:4:4. So far, OGB has not released the test-challenge set. The training set is exploited to train the models, and the validation set is used to select the best epoch. We report performance of GEM-2 and the baseline methods on the validation and test-dev sets.

**Baselines.** We compare GEM-2 with multiple baseline methods. Most baselines focus on the short-range interactions, including Graph Isomorphism Network(GIN) Xu et al. [2019], GIN-virtual, Graph Convolutional Networks (GCN) Kipf and Welling [2017] and GCN-virtual, where GIN-virtual and GCN-virtual are the ablation versions of GIN and GCN that utilize virtual node. Some baselines consider the long-range interactions, including Graph Relative Positional Encoding (GRPE) Park et al. [2022], EGT Hussain et al. [2021b] and Graphomer Ying et al. [2021].

**Results.** The results of GEM-2 and the baseline methods on dataset PCQM4Mv2 are shown in Table 2. We regard the prediction of HOMO-LUMO energy gaps as a regression problem, applying L1 loss as the loss function and Mean Absolute Error (MAE) as the evaluation metric. The reported results of GCN, GIN, GCN-virtual, GIN-virtual, GRPE and EDT are collected from the PCQM4Mv2 leaderboard<sup>4</sup>, whereas the result of Graphomer is from their paper Ying et al. [2021]. From the results, we can draw the following conclusions. First, GEM-2 achieves the best performance on the dataset, demonstrating its effectiveness in predicting the quantum chemistry properties. Second, models that directly consider the long-range interactions, i.e., GRPE, EGT, Graphomer, and GEM-2, outperform the models that focus on the short-range interactions, i.e., GCN, GIN, GCN-virtual, and GIN-virtual. The results indicate that compared with using the step-by-step message passing technique to infer the long-range interaction indirectly, directly modeling long-range interaction through full-range attention has excellent advantages in enhancing prediction accuracy.

#### 4.3 Drug Discovery Benchmark

**Dataset** LIT-PCBA Tran-Nguyen et al. [2020] is a virtual screening dataset that can be utilized to develop models for the drug discovery industry. It contains 15 protein targets as well as 9780 active compounds (positive samples) and 407,839 unique inactive compounds (negative samples) toward those targets. Predicting the activities of the candidate compounds to a protein target can be regarded as a binary classification task. Due to the large prediction variance on the tasks with only a few positive samples, we only evaluate the methods on the targets (ALDH1, FEN1, GBA, KAT2A, MAPK1, PKM2, and VDR) with more than 150 active compounds. Following the previous work Cai et al. [2022], we split the samples of each target into training and test sets at the ratio of 3:1 with asymmetric validation embedding

<sup>3</sup><https://ogb.stanford.edu/>

<sup>4</sup><https://ogb.stanford.edu/docs/lsc/leaderboards/#pcqm4mv2>

Table 3: AUC scores of GEM-2 and the baseline methods on drug discovery dataset LIT-PCBA.

	ALDH1	FEN1	GBA	KAT2A	MAPK1	PKM2	VDR	Average
No. active	7,168	369	166	194	308	546	884	-
No. inactive	137,965	355,402	296,052	348,548	62,629	245,523	355,388	-
NB Duda et al. [1973]	0.693	0.876	0.709	0.659	0.686	0.684	0.804	0.730
SVM Cortes and Vapnik [1995]	0.76	0.877	0.778	0.612	0.665	0.753	0.69	0.734
RF Liaw et al. [2002]	0.741	0.657	0.599	0.537	0.579	0.581	0.644	0.620
XGBoost Chen and Guestrin [2016]	0.75	0.888	0.83	0.5	0.593	0.737	0.782	0.726
MLP	0.756	0.901	0.777	0.595	0.708	0.719	0.794	0.750
GCN Kipf and Welling [2017]	0.73	0.897	0.735	0.621	0.668	0.636	0.773	0.723
GAT Velickovic et al. [2017]	0.739	0.888	0.776	0.662	0.697	0.724	0.78	0.752
FP-GNN Cai et al. [2022]	0.766	0.889	0.751	0.632	<b>0.771</b>	0.732	0.774	0.759
GEM-2	<b>0.790</b>	<b>0.941</b>	<b>0.848</b>	<b>0.679</b>	0.763	<b>0.785</b>	<b>0.840</b>	<b>0.807</b>

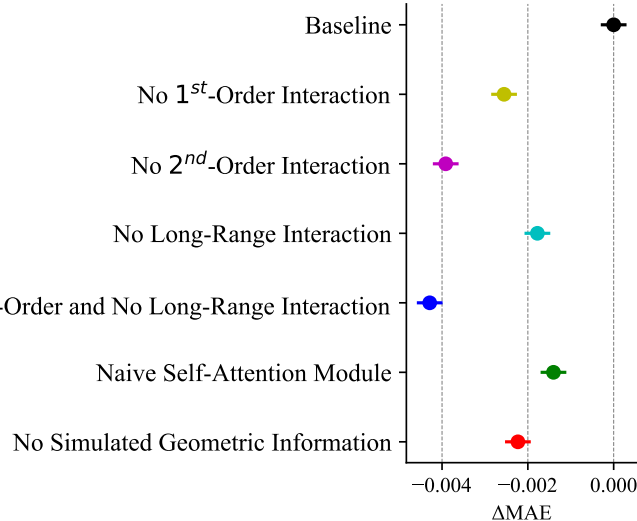


Figure 3: MAE difference compared with baseline GEM-2 (the higher the better).

(AVE) method Wallach and Heifets [2018]. Additionally, we reserve 1/9 samples in the training set as the validation set to select the best model. We evaluate the performance of the methods on the test set.

**Baselines.** We compare GEM-2 with two types of baselines. The first types of baselines are based on the traditional machine learning methods, including Naive Bayes(NB) Duda et al. [1973], support vector machine(SVM) Cortes and Vapnik [1995], random forest (RF) Liaw et al. [2002] and extreme gradient boosting (XGBoost) Chen and Guestrin [2016]. The second types of baselines are based on deep learning, containing GCN, Graph Attention Network (GAT) Velickovic et al. [2017], and FP-GNN Cai et al. [2022].

**Results.** Since each target is taken as a binary classification task, binary cross entropy is used as the loss function to optimize the models. To compare the accuracy of GEM-2 and the baseline methods, we report the area under the receiver operating characteristic curve (ROC-AUC) in Table 3. The reported results of NB, SVM, RF, XGBoost, MLP, GCN, GAT and FP-GNN are collected from Cai et al. [2022]. GEM-2 exceeds the baseline methods on almost all (6/7) the targets and achieves competitive performance with FP-GNN on target MAPK1, demonstrating the great potential of GEM-2 in drug discovery. Additionally, as we expected, the deep learning-based methods surpass those based on the traditional machine learning techniques in general.

#### 4.4 Ablation Studies

To investigate the effects of the components in GEM-2, we compare several ablation versions of GEM-2 on dataset PCQM4Mv2, as shown in Figure 3. Please refer to Appendix for the details of the implementations of the ablation versions.

- Compared with *No 1<sup>st</sup>-Order Interaction* and *No 2<sup>nd</sup>-Order Interaction* with the original GEM-2, we can conclude that both the modeling of the 1<sup>st</sup>-Order Interaction and the 2<sup>nd</sup>-Order Interaction can contribute to the accuracy of the property prediction. GEM-2 that comprehensively considers the 1<sup>st</sup>-order interaction and 2<sup>nd</sup>-order interaction is capable of further enhancing the accuracy of molecular property prediction. To our surprise, the effect of the 2<sup>nd</sup>-order interaction was more significant than that of the 1<sup>st</sup>-order interaction. We speculate that the modeling of the 2<sup>nd</sup>-order interaction contains partial information of the 1<sup>st</sup>-order interaction. Consequently, when the 1<sup>st</sup>-order interaction modeling is missing, the 2<sup>nd</sup>-order interaction modeling can somewhat fill this gap.
- From the results of *No Long-Range Interaction* and *No 2<sup>nd</sup>-Order and No Long-Range Interaction*, we can reasonably infer that compared with only considering the short-range interaction, simultaneously modeling the long-range interaction can achieve further improvement.
- We adopt the novel attention mechanisms, i.e., pair-aware atom self-attention and triangular self-attention, to learn the 1<sup>st</sup>-order interaction and the 2<sup>nd</sup>-order interaction. To verify their effectiveness, we also report the performance when using the naive attention mechanisms instead. The MAE of *Naive Self-Attention Module* is higher than that of the original GEM-2, indicating the superiority of our designed attention mechanisms.

## 5 Conclusion

Molecular property prediction serves as a fundamental task in drug and material industries, which in essence can be determined by its own electronic structure and described by the Schrödinger equation. Inspired by the calculation methods of Schrödinger equation, we clarify the importance of many-body and long-range interaction for molecular property prediction and propose GEM-2 to model the complex interaction. GEM-2 is a novel network architecture that consists of an atom track to model the full-range 1<sup>st</sup>-order interaction of atoms and a pair track to model the full-range 2<sup>st</sup>-order interaction of atom pairs. Extensive experiments were conducted to verify the effectiveness of GEM-2, which considerably outperforms other competitive methods on multiple benchmarks.

Table 4: Input features of GEM-2

Feature type	Feature	Description	Size
atom	atom type	type of atom (e.g., C, N, O), by atomic number (one-hot)	119
	aromaticity	whether the atom is part of an aromatic system (one-hot)	2
	formal charge	electrical charge (one-hot)	16
	chirality tag	CW, CCW, unspecified or other (ont-hot)	4
	degree	number of covalent bonds (one-hot)	11
	number of hydrogens	number of bonded hydrogen atoms (one-hot)	9
pair	hybridization	sp, sp <sup>2</sup> , sp <sup>3</sup> , sp <sup>3</sup> d, or sp <sup>3</sup> d <sup>2</sup> (one-hot)	5
	bond dir	begin dash, begin wedge, etc. (one-hot)	7
	bond type	single, double, triple or aromatic (one-hot)	4
	in ring	whether the bond is part of a ring (one-hot)	2
	pair hop distance	hop distance between the atom pair (float)	-
triplet	pair distance	simulated geometric distance between the atom pair (float)	-
	triplet angle	three angles of the triangle formed by triplet (float)	-
	triplet hop distance	three hop distances of atom $i$ to $j$ , $i$ to $k$ and $j$ to $k$ (int)	-

Table 5: Hyper-parameters of GEM-2

parameter name	for PCQM4Mv2	for LIT-PCBA	for Ablation Study
batch size	512	256	512
learning rate	$4 \cdot 10^{-4}$	$2 \cdot 10^{-4}$	$8 \cdot 10^{-4}$
warm-up epochs	10	10	10
epochs before learning rate decay	40	10	40
decay rate	0.5	0.5	0.5
decay epochs	10	10	10
$L$	12	12	12
$c_{\text{atom}}$	256	128	128
$c_{\text{pair}}$	256	128	128
$c_{\text{triplet}}$	256	128	128
$c_{\text{outer}}$	32	32	32
$p_{\text{atom}}$	0.05	0.05	0.05
$p_{\text{pair}}$	0.05	0.05	0.05
$N_{\text{atom}}$	8	8	8
$N_{\text{head}}^{\text{pair}}$	8	8	8

## Appendix: Detail Settings of GEM-2

All the features are extracted by RDKit. The feature list is shown in Table 4. Bond lengths and bond angles are the continuous features, while the others are the discrete features. For the continuous features, we use the Radial Basis Function Buhmann [2003] to expand each continuous value  $x$  into a vector  $e \in \mathbb{R}^M$ :

$$e_m(x) = \exp(-\gamma ||x - \mu_m||^2), \quad (2)$$

where  $\gamma$  controls the shape of the radial kernel, and we set  $\gamma = 10$ .  $\{\mu_m\}$  is a list of centers ranging from the minimum value to the maximum value of corresponding features with stride of 0.1. Besides, for the discrete features, they are converted into one-hot vectors.

The hyper-parameters of GEM-2 in various experiments are exhibited in Table 5. For the optimizer learning rate setting, we employ a linear warm-up strategy at the beginning of the training and then decay the learning rate.

## Appendix: Detail of LIT-PCBA

The description of the targets in LIT-PCBA is shown in Table 6.

Table 6: LIT-PCBA dataset

Set	Target	Actives	Inactives
ADRB2	Beta2 adrenergic receptor	17	312,483
ALDH1	Aldehyde dihydrogenase 1	7,168	137,965
ESR_ago	Estrogen receptor $\alpha$	13	5,583
ESR_antago	Estrogen receptor $\alpha$	102	4,948
FEN1	FLAP Endonuclease	369	355,402
GBA	Glucocerebrosidase	166	296,052
IDH1	Isocitrate dihydrogenase	39	362,049
KAT2A	Histone acetyltransferase KAT2A	194	348,548
MAPK1	Mitogen-activated protein kinase 1	308	62,629
MTORC1	Mechanistic target of rapamycin	97	32,972
OPRK1	Kappa opioid receptor	24	269,816
PKM2	Pyruvate kinase muscle isoform 2	546	245,523
PPARG	Peroxisome proliferator-activated receptor $\gamma$	27	5,211
TP53	Cellular tumor antigen p53	79	4,168
VDR	Vitamin D receptor	884	355,388

## Appendix: Ablation Versions of GEM-2

The implementation of the ablation versions of GEM-2 is described as follows:

- *No 1<sup>st</sup>-Order Interaction.* It removes pair-aware atom self-attention in the atom-level track. Mean pooling is applied to the pair representations to predict the properties.
- *No 2<sup>nd</sup>-Order Interaction.* It removes triangular self-attentions from the pair-level track.
- *No Long-Range Interaction.* When calculating the attention weights, the interactions between the atoms that are spatially far away are masked.
- *No 2<sup>nd</sup>-Order and No Long-Range Interaction.* It combines *No 2<sup>nd</sup>-Order Interaction* and *No Long-Range Interaction*.
- *Naive Self-Attention Module.* In the pair-aware atom self-attention, the pair representation is taken as the bias and added to the attention weights. In the triangular self-attentions, the triplet representation is taken as the bias and added to the attention weights.

## References

Maho Nakata and Tomomi Shimazaki. Pubchemqc project: a large-scale first-principles electronic structure database for data-driven chemistry. *Journal of chemical information and modeling*, 57(6):1300–1308, 2017.

Nicolò Defenu, Tobias Donner, Tommaso Macrì, Guido Pagano, Stefano Ruffo, and Andrea Trombettoni. Long-range interacting quantum systems. (arXiv:2109.01063), Sep 2021. doi:10.48550/arXiv.2109.01063. URL <http://arxiv.org/abs/2109.01063>. arXiv:2109.01063 [cond-mat, physics:quant-ph].

Kieron Burke and Lucas O. Wagner. Dft in a nutshell. *International Journal of Quantum Chemistry*, 113(2):96–101, 2013. ISSN 1097-461X. doi:10.1002/qua.24259.

Roberto Peverati and Donald G. Truhlar. Quest for a universal density functional: the accuracy of density functionals across a broad spectrum of databases in chemistry and physics. *Philosophical Transactions of the Royal Society A: Mathematical, Physical and Engineering Sciences*, 372(2011):20120476, Mar 2014. doi:10.1098/rsta.2012.0476.

Luke W. Bertels, Joonho Lee, and Martin Head-Gordon. Polishing the gold standard: The role of orbital choice in ccisd(t) vibrational frequency prediction. *Journal of Chemical Theory and Computation*, 17(2):742–755, Feb 2021. ISSN 1549-9618. doi:10.1021/acs.jctc.0c00746.

Igor Ying Zhang and Andreas Grüneis. Coupled cluster theory in materials science. *Frontiers in Materials*, 6, 2019. ISSN 2296-8016. URL <https://www.frontiersin.org/articles/10.3389/fmats.2019.00123>.

John Jumper, Richard Evans, Alexander Pritzel, Tim Green, Michael Figurnov, Olaf Ronneberger, Kathryn Tunyasuvunakool, Russ Bates, Augustin Žídek, Anna Potapenko, et al. Highly accurate protein structure prediction with alphafold. *Nature*, 596(7873):583–589, 2021.

Chengxuan Ying, Tianle Cai, Shengjie Luo, Shuxin Zheng, Guolin Ke, Di He, Yanming Shen, and Tie-Yan Liu. Do transformers really perform badly for graph representation? *Advances in Neural Information Processing Systems*, 34: 28877–28888, 2021.

Vijay Prakash Dwivedi and Xavier Bresson. A generalization of transformer networks to graphs. *CoRR*, abs/2012.09699, 2020. URL <https://arxiv.org/abs/2012.09699>.

Md. Shamim Hussain, Mohammed J. Zaki, and Dharmashankar Subramanian. Edge-augmented graph transformers: Global self-attention is enough for graphs. *CoRR*, abs/2108.03348, 2021a. URL <https://arxiv.org/abs/2108.03348>.

Tomasz Danel, Przemysław Spurek, Jacek Tabor, Marek Smieja, Lukasz Struski, Agnieszka Slowik, and Lukasz Maziarka. Spatial graph convolutional networks. In Haiqin Yang, Kitsuchart Pasupa, Andrew Chi-Sing Leung, James T. Kwok, Jonathan H. Chan, and Irwin King, editors, *Neural Information Processing - 27th International Conference, ICONIP 2020, Bangkok, Thailand, November 18-22, 2020, Proceedings, Part V*, volume 1333 of *Communications in Computer and Information Science*, pages 668–675. Springer, 2020. doi:10.1007/978-3-030-63823-8\_76. URL [https://doi.org/10.1007/978-3-030-63823-8\\_76](https://doi.org/10.1007/978-3-030-63823-8_76).

Zhaoping Xiong, Dingyan Wang, Xiaohong Liu, Feisheng Zhong, Xiaozhe Wan, Xutong Li, Zhaojun Li, Xiaomin Luo, Kaixian Chen, Hualiang Jiang, and Mingyue Zheng. Pushing the boundaries of molecular representation for drug discovery with the graph attention mechanism. *Journal of Medicinal Chemistry*, 63(16):8749–8760, 2020. doi:10.1021/acs.jmedchem.9b00959. URL <https://doi.org/10.1021/acs.jmedchem.9b00959>. PMID: 31408336.

Lukasz Maziarka, Tomasz Danel, Slawomir Mucha, Krzysztof Rataj, Jacek Tabor, and Stanisław Jastrzebski. Molecule attention transformer. *CoRR*, abs/2002.08264, 2020. URL <https://arxiv.org/abs/2002.08264>.

Kristof Schütt, Pieter-Jan Kindermans, Huziel Enoc Sauceda Felix, Stefan Chmiela, Alexandre Tkatchenko, and Klaus-Robert Müller. Schnet: A continuous-filter convolutional neural network for modeling quantum interactions. In Isabelle Guyon, Ulrike von Luxburg, Samy Bengio, Hanna M. Wallach, Rob Fergus, S. V. N. Vishwanathan, and Roman Garnett, editors, *Advances in Neural Information Processing Systems 30: Annual Conference on Neural Information Processing Systems 2017, December 4-9, 2017, Long Beach, CA, USA*, pages 991–1001, 2017. URL <https://proceedings.neurips.cc/paper/2017/hash/303ed4c69846ab36c2904d3ba8573050-Abstract.html>.

Jintang Li, Kun Xu, Liang Chen, Zibin Zheng, and Xiao Liu. Graphgallery: A platform for fast benchmarking and easy development of graph neural networks based intelligent software. In *43rd IEEE/ACM International Conference on Software Engineering: Companion Proceedings, ICSE Companion 2021, Madrid, Spain, May 25-28, 2021*, pages 13–16. IEEE, 2021. doi:10.1109/ICSE-Companion52605.2021.00024. URL <https://doi.org/10.1109/ICSE-Companion52605.2021.00024>.

Johannes Klicpera, Janek Groß, and Stephan Günnemann. Directional message passing for molecular graphs. In *8th International Conference on Learning Representations, ICLR 2020, Addis Ababa, Ethiopia, April 26-30, 2020*. OpenReview.net, 2020. URL <https://openreview.net/forum?id=B1eWbxStPH>.

Kevin Yang, Kyle Swanson, Wengong Jin, Connor W. Coley, Philipp Eiden, Hua Gao, Angel Guzman-Perez, Timothy Hopper, Brian Kelley, Miriam Mathea, Andrew Palmer, Volker Settels, Tommi S. Jaakkola, Klavs F. Jensen, and Regina Barzilay. Analyzing learned molecular representations for property prediction. *J. Chem. Inf. Model.*, 59(8):3370–3388, 2019. doi:10.1021/acs.jcim.9b00237. URL <https://doi.org/10.1021/acs.jcim.9b00237>.

Zeren Shui and George Karypis. Heterogeneous molecular graph neural networks for predicting molecule properties. In Claudia Plant, Haixun Wang, Alfredo Cuzzocrea, Carlo Zaniolo, and Xindong Wu, editors, *20th IEEE International Conference on Data Mining, ICDM 2020, Sorrento, Italy, November 17-20, 2020*, pages 492–500. IEEE, 2020. doi:10.1109/ICDM50108.2020.00058. URL <https://doi.org/10.1109/ICDM50108.2020.00058>.

Xiaomin Fang, Lihang Liu, Jieqiong Lei, Donglong He, Shanzhuo Zhang, Jingbo Zhou, Fan Wang, Hua Wu, and Haifeng Wang. Geometry-enhanced molecular representation learning for property prediction. *Nature Machine Intelligence*, 4(2):127–134, 2022.

Guohao Li, Chenxin Xiong, Ali K. Thabet, and Bernard Ghanem. Deepgcn: All you need to train deeper gcns. *CoRR*, abs/2006.07739, 2020. URL <https://arxiv.org/abs/2006.07739>.

Weihua Hu, Bowen Liu, Joseph Gomes, Marinka Zitnik, Percy Liang, Vijay S. Pande, and Jure Leskovec. Strategies for pre-training graph neural networks. In *8th International Conference on Learning Representations, ICLR 2020, Addis Ababa, Ethiopia, April 26-30, 2020*. OpenReview.net, 2020. URL <https://openreview.net/forum?id=HJ1WWJSFDH>.

Jianwen Chen, Shuangjia Zheng, Ying Song, Jiahua Rao, and Yuedong Yang. Learning attributed graph representations with communicative message passing transformer. *CoRR*, abs/2107.08773, 2021. URL <https://arxiv.org/abs/2107.08773>.

Devin Kreuzer, Dominique Beaini, William L. Hamilton, Vincent Létourneau, and Prudencio Tossou. Rethinking graph transformers with spectral attention. In Marc’Aurelio Ranzato, Alina Beygelzimer, Yann N. Dauphin, Percy Liang, and Jennifer Wortman Vaughan, editors, *Advances in Neural Information Processing Systems 34: Annual Conference on Neural Information Processing Systems 2021, NeurIPS 2021, December 6-14, 2021, virtual*, pages 21618–21629, 2021. URL <https://proceedings.neurips.cc/paper/2021/hash/b4fd1d2cb085390fbbaade65e07876a7-Abstract.html>.

Diederik P. Kingma and Jimmy Ba. Adam: A method for stochastic optimization. In Yoshua Bengio and Yann LeCun, editors, *3rd International Conference on Learning Representations, ICLR 2015, San Diego, CA, USA, May 7-9, 2015, Conference Track Proceedings*, 2015. URL <http://arxiv.org/abs/1412.6980>.

Keyulu Xu, Weihua Hu, Jure Leskovec, and Stefanie Jegelka. How powerful are graph neural networks? In *7th International Conference on Learning Representations, ICLR 2019, New Orleans, LA, USA, May 6-9, 2019*. OpenReview.net, 2019. URL <https://openreview.net/forum?id=ryGs6iA5Km>.

Thomas N. Kipf and Max Welling. Semi-supervised classification with graph convolutional networks. In *5th International Conference on Learning Representations, ICLR 2017, Toulon, France, April 24-26, 2017, Conference Track Proceedings*. OpenReview.net, 2017. URL <https://openreview.net/forum?id=SJU4ayYg1>.

Wonpyo Park, Woonggi Chang, Donggeon Lee, and Juntae Kim. Graph self-attention for learning graph representation with transformer. *arXiv preprint arXiv:2201.12787*, 2022.

Md Shamim Hussain, Mohammed J Zaki, and Dharmashankar Subramanian. Edge-augmented graph transformers: Global self-attention is enough for graphs. *arXiv preprint arXiv:2108.03348*, 2021b.

Viet-Khoa Tran-Nguyen, Célien Jacquemard, and Didier Rognan. Lit-pcba: An unbiased data set for machine learning and virtual screening. *Journal of chemical information and modeling*, 60(9):4263–4273, 2020.

Hanxuan Cai, Huimin Zhang, Duancheng Zhao, Jingxing Wu, and Ling Wang. Fp-gnn: a versatile deep learning architecture for enhanced molecular property prediction. *arXiv preprint arXiv:2205.03834*, 2022.

Izhar Wallach and Abraham Heifets. Most ligand-based classification benchmarks reward memorization rather than generalization. *Journal of chemical information and modeling*, 58(5):916–932, 2018.

Richard O Duda, Peter E Hart, et al. *Pattern classification and scene analysis*, volume 3. Wiley New York, 1973.

Corinna Cortes and Vladimir Vapnik. Support-vector networks. *Machine learning*, 20(3):273–297, 1995.

Andy Liaw, Matthew Wiener, et al. Classification and regression by randomforest. *R news*, 2(3):18–22, 2002.

Tianqi Chen and Carlos Guestrin. Xgboost: A scalable tree boosting system. In *Proceedings of the 22nd acm sigkdd international conference on knowledge discovery and data mining*, pages 785–794, 2016.

Petar Velickovic, Guillem Cucurull, Arantxa Casanova, Adriana Romero, Pietro Liò, and Yoshua Bengio. Graph attention networks. *arXiv preprint*, abs/1710.10903, 2017. URL <http://arxiv.org/abs/1710.10903>.

Martin D Buhmann. *Radial basis functions: theory and implementations*, volume 12. Cambridge university press, 2003.